



Characteristic results and prospects of the 13Cr–1W–0.3Ti–0.3Y₂O₃ ODS steel

Ch.Ch. Eiselt*, M. Klimenkov, R. Lindau, A. Möslang

Forschungszentrum Karlsruhe/IMF I, P.O. Box 3640, 72061 Karlsruhe, Germany

A B S T R A C T

For specific blanket and divertor applications in future fusion power reactors a replacement of presently considered reduced activation ferritic martensitic (RAFM) steels as structural material by suitable oxide dispersion strengthened (ODS) ferritic martensitic steels would allow a substantial increase of the operating temperature from ~550 °C to about 650 °C. Temperatures above 700 °C in the He cooled modular divertor concept necessitates the use of ferritic (RAF) ODS steels, which are not limited by a phase transition. Therefore a 13Cr–1W–0.3Ti–0.3Y₂O₃ ferritic ODS steel is being developed, using an Attritor with varying milling parameters. Afterwards the mechanically alloyed powders were encapsulated, sealed and consolidated in a hot isostatic press device. In this work, the effects of several parameter variations on the microstructure of the produced ferritic ODS-alloys, analysed by optical microscopy (OM) and high resolution TEM, as well as results of conducted mechanical tests are presented.

© 2008 Elsevier B.V. All rights reserved.

1. Introduction

Within a future global energy scenario fusion power plants should play a decisive role for an environmentally friendly energy supply. An important issue for this mission is the availability of suitable structural materials, which can stand the upcoming stresses, for example surface heat fluxes, neutron radiation damages, integral dose rates and different operational modes of the reactors. Thereby materials are subjected to a complicated interaction of coolant influences and high temperature creep deformations for many years.

The most demanding ‘in vessel’ component in a future fusion power plant is presently a helium gas cooled divertor having a surface heat flux of typically 10 MW/m². However, even in the non-irradiated condition there is no structural material right now, that meets at the same time at 1200 K a thermal conductivity λ of ≥ 100 W/mK, a creep rupture strength $\sigma_{R20000h}$ of ≥ 55 MPa, and a ductile to brittle transition temperature of < 600 °C. As there is no realistic alternative within the international fusion materials community, the design is presently based on dispersion strengthened structural materials like ferritic ODS steels of type 12–14CrW–Y₂O₃.

Based on earlier very promising results with the ODS-Eurofer alloy [1] and perspectives [2], an RAF-ODS-alloy with a pure ferritic matrix shall be developed, to once more substantially extend the upper temperature limit of 650 °C of today’s RAFM steels by avoiding a phase transition. The low tungsten content of only 1 wt% keeps the option open to this ODS steel potentially also for First

Wall applications in helium cooled pebble bed blankets, as it would not compromise the tritium production rate by strong neutron capture.

2. Experimental

The development concentrates mainly on the 13Cr–1W ferritic ODS steel, using the powder-metallurgical route for the alloy production. After establishing an optimum processing route, 13Cr ferritic steel powder together with 0.3 wt% Y₂O₃ and 0.3 wt% Ti powder was ball milled in an argon inert gas atmosphere, using a ZOZ Attritor Simoloyer CM01, under varying milling parameters, such as milling time and variable rotational frequencies. Equally the tungsten content is limited to 1 wt%. A higher amount of tungsten inside the material would lead to a higher capturing rate of neutrons in the fusion process, resulting in a lower Tritium breeding ratio. Afterwards the milled powders were filled and predensified in a specially designed HIP pressure capsule. The capsule is degassed at 400 °C, sealed and consolidated in a HIP (hot isostatic press) device using the following parameters: $p_{hip} = 1000$ bar, $T_{hip} = 1150$ °C, $t_{hip} = 2$ h. Then samples were taken from the hipped material. After polishing and etching these were analysed by optical microscopy (OM) and raster electron microscopy (REM).

Furthermore samples for transmission electron microscopy (TEM) were cut from the hipped material and mechanically thinned to a thickness of ~130–150 μ m. From these discs, TEM-samples of 3 mm diameter were punched and electro-polished in a Tenupol device using 20% H₂SO₄ and 80% CH₃OH as electrolyte. In addition to that these samples were cleaned for a few minutes with an Ar ion beam at low angle in a precise ion polishing system made by Gatan Ltd. For the conducted analyses two different types

* Corresponding author.

E-mail address: Charles.eiselt@imf.fzk.de (Ch.Ch. Eiselt).

of TEM microscopes were used: a Philips CM30 (300 kV) and a FEI TECNAI-20F.

3. Results

3.1. Microstructural investigations

The investigated material was manufactured by using different milling times, but identical HIP-parameters, as described before. Fig. 1 shows optical micrographs (OM) in the as HIPped state for 4 h, for 10 h and for 28 h milling time, each at 1200 rpm and according to the same HIP-parameters. In all images areas of dark contrast can be seen in the matrix. Those are pores Fig. 1.

Fig. 2(a)–(c) shows bright field TEM images for the same specimens and parameter sets as Fig. 1.

Those TEM images reveal a grain structure, which can be divided into two well distinguishable areas: an area with nanometer sized grains, varying from 20 nm to 500 nm and another area with a classical ferritic grain structure from 1 μm to 8 μm . The nanometer grains are roundly shaped, while the micrometer grains have also elongated appearances. This can be interpreted as a bimodal grain size distribution.

After 4 h of milling mainly nanometer sized grains with very few embedded micrometer-sized grains are visible. Increasing the milling time to 10 h shows an enlargement of the micrometer grain areas, resulting in a mixture of both area types. A further increase to 28 h of milling leads to a strong reduction of the nano-structured areas. Fig. 2(c) shows for example, that the nano-sized areas exist only in the upper part.

These characteristics were described elsewhere [3–5] Fig. 2.

It can be seen, that the compaction of the milled powders in the HIP-cycle was successfully conducted and only a small porosity (<1%) remained in the material.

In addition the sample of 10 h milling time was heat treated ($T = 1050\text{ }^\circ\text{C}$, $t = 30\text{ min}$, 1 h, 2 h, 3 h, and 4 h), to analyse the behaviour of the bimodality in detail. At all temperatures the bimodality remained and no significant change in the microstructure was detected, underlining the stability of this phenomenon.

Furthermore the distribution and morphology of ODS-particle characteristics were analysed. In Fig. 2(d)–(f) high angle annular dark field (HAADF) images of the same samples as in Figs. 1 and 2 are presented. ODS-particles can be identified as round spots of dark contrast. Fig. 2(d) contains ODS-particles with sizes of 10–50 nm located in the middle of the image. Taking into account the bimodality in grain sizes, it can be stated, that mainly 3–4 nm ODS-particles can be found in the micrometer grains, while 12–20 nm particles appear in the nanometer grains, especially on the grain boundaries (see Fig. 2(e)). Additionally in Fig. 2(f) larger numbers of particles with $d \geq 20\text{ nm}$ can be seen. Near those, the 3–4 nm sized ODS-particles were completely missing. The particles were located rather at the grain boundaries than within the grains.

Already 4 h milling time were sufficient to form nanometer sized ODS-particles after the HIP-process. But during the analyses several locations on the sample without any ODS-particles were found, so that a general inhomogeneous distribution is assumed.

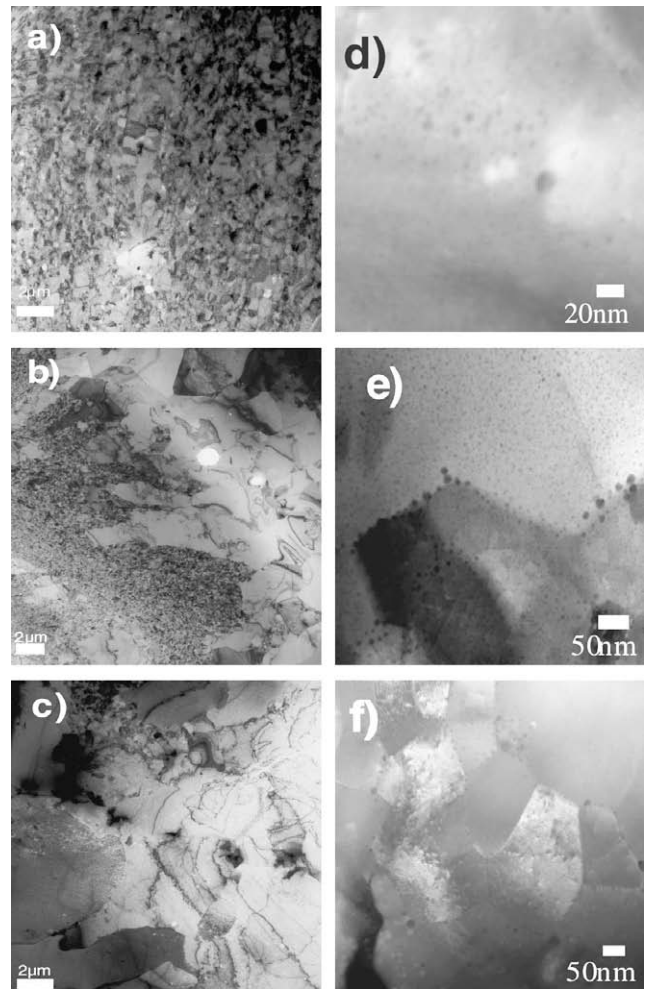


Fig. 2. BFTEM images (a), (b), (c) and HAADF images (d), (e), (f) of the 13Cr-1W-0.3Ti-0.3Y₂O₃ ODS-alloy; (a) + (d) 4 h, (b) + (e) 10 h, and (c) + (f) 28 h milling time; HIP-parameters: $p_{\text{hip}} = 1000\text{ bar}$, $T_{\text{hip}} = 1150\text{ }^\circ\text{C}$, $t_{\text{hip}} = 2\text{ h}$.

After 10 h (see Fig. 2(e)) the ODS-particle distribution was a lot more homogeneous, because actionally no sample areas existed, where no ODS-particles were detected. Twenty-eight hours of milling resulted also in ODS-particle formation, but the dispersion was not equally homogeneous Fig. 3.

Fig. 3(a) contains a further HAADF image of nano-structured grains in a sample of 10 h milling time and identical HIP-parameters together with the corresponding elemental mapping for characteristic elements of the square marked region: iron 3b, chromium 3c, yttrium 3d, titanium 3e, oxygen 3f and argon 3g. A bright contrast indicates a high elemental concentration. Because of the correspondence of the bright contrasted dots in the HAADF image with the yttrium, titanium and oxygen signals, while iron is absent at the same positions, the ODS-particle formation can be clearly verified in the 13Cr-1W-0.3Ti-0.3Y₂O₃ ferritic ODS-alloy. The analyses of Cr-map (Fig. 3(c)) shows a chromium enrichment on

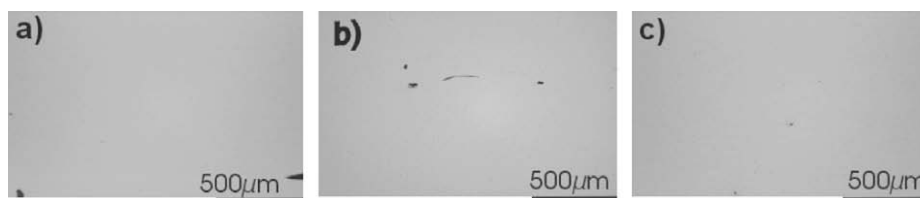


Fig. 1. Characterization of polished samples of the 13Cr-1W-0.3Ti-0.3Y₂O₃ ODS-alloy by optical microscopy (OM); (a) 4 h, (b) 10 h, and (c) 28 h.

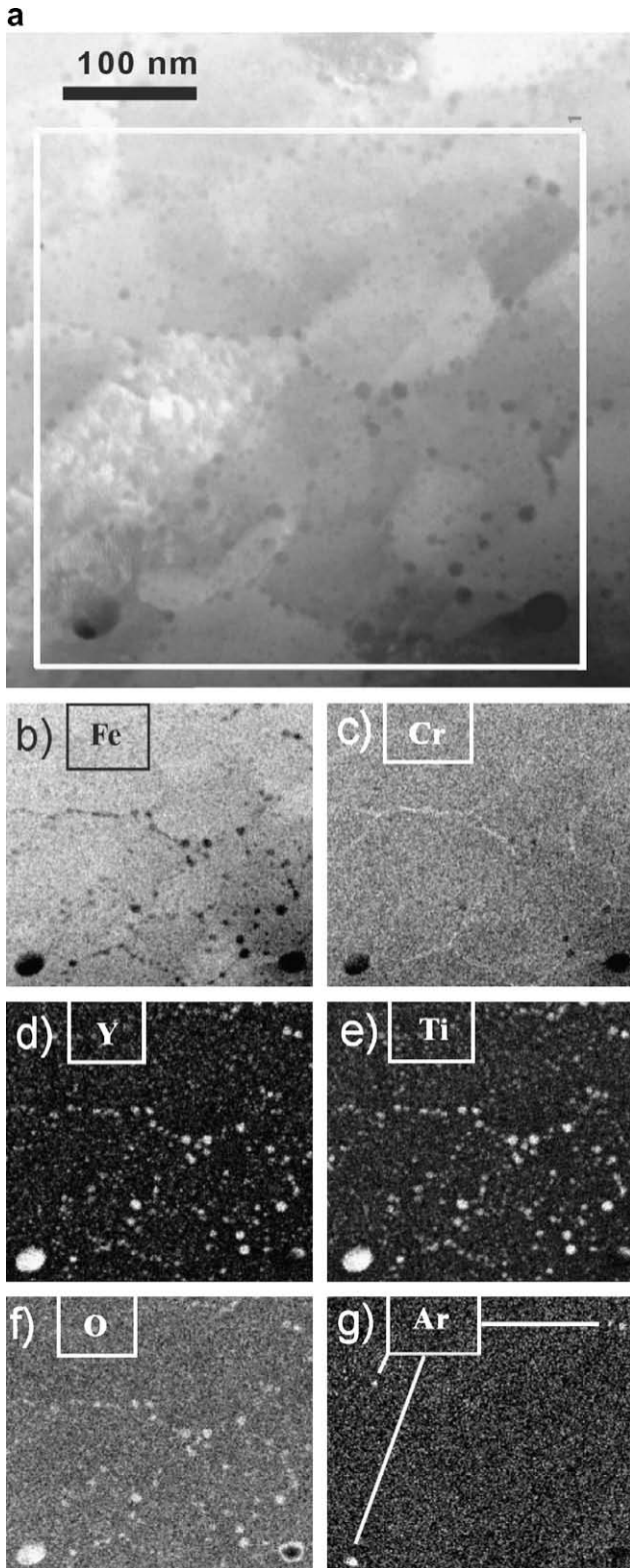


Fig. 3. HAADF image (a) and corresponding spatial elemental maps (b)–(g) for characteristic elements of the 13Cr–1W–0.3Ti–0.3Y₂O₃ ODS-alloy after 10 h milling time; HIP-parameters $p_{\text{hip}} = 1000$ bar, $T_{\text{hip}} = 1150$ °C, $t_{\text{hip}} = 2$ h.

the grain boundaries. In addition three argon filled bubbles, marked by arrows in Fig. 3(g), were detected in connection with ODS-particles, coming from the milling atmosphere. This behaviour has already been stated elsewhere [6]. Generally ODS-particle formation could hereby be confirmed and the purity of the final

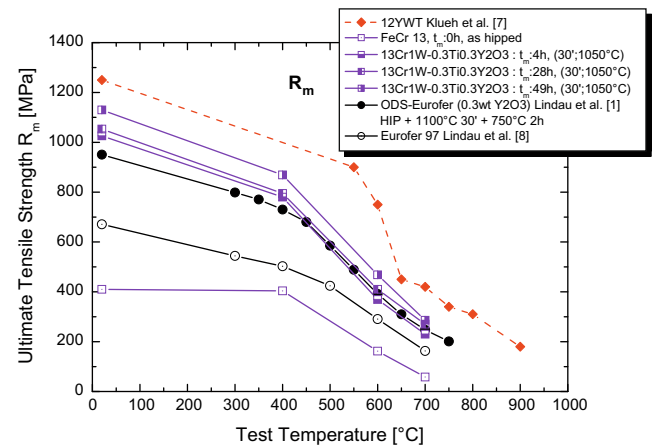


Fig. 4. Ultimate tensile strengths of 13Cr–1W–0.3Ti–0.3Y₂O₃. Manufactured with alternating milling times and following HIP-parameters: $p_{\text{hip}} = 1000$ bar, $T_{\text{hip}} = 1150$ °C, $t_{\text{hip}} = 2$ h; comparison with Eurofer 97, ODS-Eurofer and 12YWT as reference alloys.

material could be judged, by displaying the relevant elements Fig. 4.

3.2. Mechanical tests

In addition to TEM-analyses several mechanical tests of the produced alloys were carried out. Fig. 4 contains the ultimate tensile strengths R_m of following alloys: three types of the 13Cr–1W–0.3Ti–0.3Y₂O₃ alloys are displayed, differing in the milling times and rotational frequencies: the 49 h mechanically alloyed powder was milled with 500 rpm instead of 1200 rpm as the other two ferritic ODS-alloys to minimize contamination. All of them got an additional heat treatment (30'; 1050 °C) after the HIP-process. FeCr13 specimen was produced from basic powders without any mechanical alloying or heat treatments and were HIPped with the same parameter sets. The data of 12YWT [7] and ODS-Eurofer [1] serve as a reference for comparison of the different ODS-alloy types. It can be seen that a significant strength increase also occurs for the three ferritic ODS-alloys compared to the basic unmilled FeCr13 material, like it takes place with ODS-Eurofer and Eurofer 97 [8]. This increase is even stronger for the ferritic ODS-alloys. At the investigated temperatures, the manufactured ferritic ODS-alloys behave similarly to ODS-Eurofer, with only slightly different R_m values. The highest R_m levels at the shown temperatures has the 12YWT ODS-alloy [7].

The total elongation A of the ferritic ODS-alloys in the conducted mechanical tests is smaller than that of ODS-Eurofer.

Furthermore Charpy impact tests for the specimen produced with the same parameter sets have been executed. Hereby the ferritic ODS-alloys have a low ductility at the investigated temperatures.

Generally the results of the mechanical tests of the ferritic ODS-alloys are very promising, but high temperature ductility and impact behaviour are not yet satisfactory. It is expected, that thermo-mechanical treatments such as rolling or extrusion, which are under execution, shall improve the impact energy levels.

4. Summary and conclusion

Using the powder-metallurgical production route, 13Cr–1W–0.3Ti–0.3Y₂O₃ ferritic ODS-alloys has been produced under varying milling times, rotational frequencies and equal HIP-parameters. In addition mechanical tests with these produced ferritic ODS-alloys have been carried out.

The bimodal grain size distribution, once created, is very stable. But depending on the milling time and rotational frequencies, there are fluctuations. Obviously the influence of HIP-parameters are limited here. One reason for the bimodality could be the ability of ODS-particles to pin grain boundaries and therefore prohibiting recrystallization. But this phenomenon is not appearing homogeneously throughout the manufactured alloys and needs further investigation.

References

- [1] R. Lindau, M. Klimenkov, A. Möslang, M. Rieth, B. Schedler, J. Schröder, A. Schwaiger, in: Proceedings of the 16th International Plansee Seminar, Reutte, Austria, 2005, p. 545.
- [2] S. Ukai, M. Fujiwara, J. Nucl. Mater. 307–311 (2002) 749.
- [3] P. Miao, G.R. Odette, T. Yamato, M. Alinger, D. Hoelzer, D. Gragg, J. Nucl. Mater. 367–370 (2007) 208.
- [4] H. Kishimoto, M.J. Alinger, G.R. Odette, T. Yamamoto, J. Nucl. Mater. 329–333 (2004) 369.
- [5] Z. Oksiuta, N. Baluc, J. Nucl. Mater. 374 (2008) 178.
- [6] M. Klimiankou, R. Lindau, A. Möslang, J. Nucl. Mater. 329–333 (2004) 347.
- [7] R.L. Klueh, J.P. Shingledecker, R.W. Swindeman, D.T. Hoelzer, J. Nucl. Mater. 341 (2005) 103.
- [8] R. Lindau, M. Schirra, Fus. Eng. Des. 58–59 (2001) 781.